Int J Earth Sci (Geol Rundsch) (2012) 101:937–950
DOI 10.1007/s00531-011-0700-0

ORIGINAL PAPER

Recognition of early Carboniferous alkaline granite in the southern Altai orogen: post-orogenic processes constrained by U–Pb zircon ages, Nd isotopes, and geochemical data

Ying Tong · Tao Wang · Wolfgang Siebel · Da-Wei Hong · Min Sun

Received: 16 July 2010 / Accepted: 8 July 2011 / Published online: 5 August 2011

Abstract The Altai orogen forms the southern part of the Central Asian Orogenic Belt (CAOB), the world's largest accretionary orogen. However, its tectonic evolution, particularly during the late Paleozoic, is still not well understood. U–Pb zircon analyses for the Bulgen alkaline granite yield crystallization ages of 358 ± 4 Ma (SHRIMP) and 354 ± 4 Ma (LA-ICP-MS). These ages are significantly younger than published emplacement ages for subduction/collision-related syn-orogenic granitoids (460–375 Ma) in this region. The Bulgen granite has high SiO_2, total alkalis, rare earth elements, HFSE (Th, Zr, Hf, Nb, and Ce), and low Ba, Sr with pronounced negative anomalies in Eu, Ba, Sr, P, and Ti, showing a clear A-type geochemical signature. The granite records high $\varepsilon Nd(t)$ values of +6.3 to +6.4 and young model ages (T_{DM}) of ca. 600 Ma. The Bulgen alkaline granite is largely undeformed as opposed to the early-middle Paleozoic counterparts, which form elongated deformed bodies parallel to the prevailing tectonic fabric (NW direction). Available data suggest that magmatism in the southern Altai region evolved from early-middle Paleozoic I-type tholeiitic and calc-alkaline granitoids to late Paleozoic A-type alkaline granitoids. The high $\varepsilon Nd(t)$ values of the Bulgen alkaline granite indicate a homogeneous juvenile mantle source, whereas the early-middle Paleozoic granitoids are characterized by lower and more variable $\varepsilon Nd(t)$ values (−2.6 to +4.2). These differences provide an important insight into the late Paleozoic orogenic processes of the Chinese Altai and indicate a significant change of the tectonic regime from a syn-orogenic regional compression setting to a post-orogenic extensional one. Major tectonic movements in this region ceased after the early Carboniferous.

Keywords Zircon U–Pb · Chinese Altai · Alkaline granite · Post-orogenic · Central Asian Orogenic Belt

Y. Tong (✉) · T. Wang · D.-W. Hong
Institute of Geology, Chinese Academy of Geological Sciences, Baiwanzhuang Road 26, Beijing 100037, China
e-mail: yingtong@cags.ac.cn

Y. Tong · W. Siebel
Institute of Geosciences, University of Tübingen, 72074 Tübingen, Germany

M. Sun
Department of Earth Sciences, The University of Hong Kong, Pokfulam Road, Hong Kong, China

Introduction

The Central Asian Orogenic Belt (CAOB, Jahn et al. 2000), also termed Altaid Tectonic Collage, or Altaids (Sengör et al. 1993; Yakubchuk 2004; Kovalenko et al. 2004; Windley et al. 2007), is the world's largest Paleozoic to Mesozoic accretionary orogen (Sengör et al. 1993; Jahn et al. 2000; Hong et al. 2004; Jahn 2004). It extends southwards from the Siberian craton to the North China and Tarim cratons, and eastwards from the Urals to the Pacific Ocean (Fig. 1, inset). Formation of this orogenic belt started at *c*. 1.0 Ga (Khain et al. 2002; Kovalenko et al. 2004; Windley et al. 2007) and the tectonic evolution continued until the Permian, when the Palaeo-Asian ocean closed along the Solonker suture (Xiao et al. 2003, 2008a). Sengör et al. (1993) proposed that the Altaids formed by successive fore-arc accretion of a long-lived, single subduction system. Recent studies, however, have revealed that a single subduction-accretion model is not sufficient to explain the complexity of the belt (e.g., Coleman 1989; Mossakovsky et al. 1993; Hu et al. 2000; Windley et al.

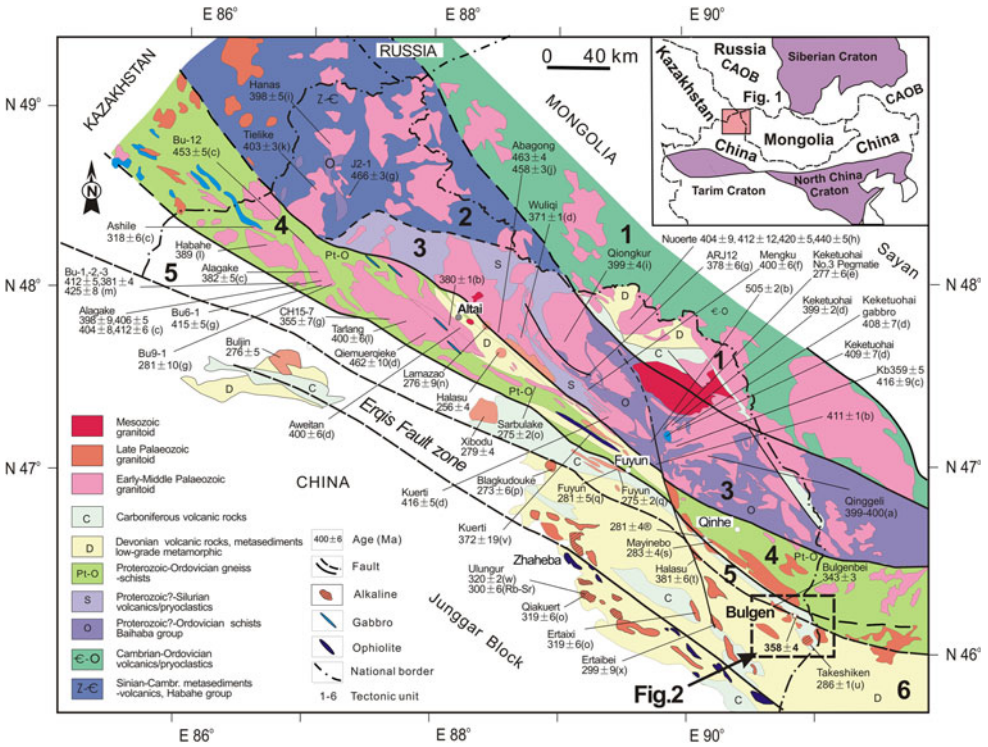

Fig. 1 Generalized geological map of the Chinese Altai. Tectonic subdivision is modified from Windley et al. (2002) and Xiao et al. (2004). Important Paleozoic plutons are marked by their names and zircon ages. Data sources: *a* Wang et al. (1998); *b* Windley et al. (2002); *c* Yuan et al. (2007); *d* Wang et al. (2006); *e* Wang et al. (2007); *f* Yang et al. (2008); *g* Sun et al. (2009a); *h* Lou (1997); *i* Tong et al. (2007); *j* Liu et al. (2008b); *k* Tong et al. (2005); *l* Yuan et al. (2006); *m* Sun et al. (2008); *n* Wang et al. (2005); *o* Sun et al. (2009b); *p* Han et al. (2006); *q* Tong et al. (2006a); *r* Zhou et al. (2007b); *s* Zhou et al. (2007a); *t* Zhang et al. (2006); *u* Tong et al. (2006b); *v* Zhang et al. (2003); *w* Liu et al. (1996); Han et al. (1997); *x* Li et al. (2004); and others are our unpublished data

2002; Badarch et al. 2002). Therefore, one of the major questions is whether a long-lasting continuous or an episodic evolution process accomplished the accretion of the CAOB.

The Altai orogen makes up of the southern part of the CAOB and includes the Altai mountains in Mongolia, China, Russia, and Kazakhstan. The Chinese Altai mountains are a key area for understanding the development of the accretion orogen in the CAOB. This region is characterized by major granitoids and granitic gneisses, which occupy more than 70% of the area (Windley et al. 2002). Based on previous Rb–Sr, K–Ar, and Ar–Ar ages (e.g., Zou et al. 1989; Zhao et al. 1993; He et al. 1994), the granitoids were considered to have been emplaced during the late Paleozoic. Consequently, this belt was considered as a late Paleozoic ("Hercynian") orogen. However, new U–Pb zircon ages demonstrate that most plutons already formed during the early-middle Paleozoic (460–375 Ma) (Fig. 1, e.g., Tong et al. 2005, 2007; Wang et al. 2006; Yuan et al. 2007; Yang et al. 2008; Sun et al. 2008, 2009a). Wang et al. (2006) and Long et al. (2007, 2010) proposed a new tectonic model for the early-middle Paleozoic syn-orogenic evolution, which provides a better explanation for the subduction and accretion processes through the Paleozoic. However, a number of issues regarding the late-stage tectonic processes during the late Paleozoic evolution of the Altai orogen remain unclear. One issue is whether the early-middle Paleozoic syn-orogenic processes prevailed until the late Paleozoic (e.g., Xiao et al. 2006, 2008b; Chen et al. 2006; Long et al. 2006; Hu et al. 2006; Cai et al. 2007) or changed into a post-orogenic setting (Mao et al. 2006; Tong et al. 2006a, b). One approach to address this problem is to study the alkaline granites in the region. In this paper, we present new SHRIMP and LA-ICP-MS U–Pb zircon data for the Bulgen alkaline granite. Combined with petrological and geochemical data, these provide important constraints on the tectonic evolution of the Chinese Altai.

Geological setting

The Chinese Altai is located between the Sayan orogenic belt in the north and the Junggar block in the south (Fig. 1). It consists of numerous terranes (Windley et al. 2002) or tectonic units (He et al. 1990; Li et al. 2003; Xiao et al. 2004) and can be divided into three units (Wang et al. 2006, 2009). The northern unit (terrane 1) consists of middle-late Devonian andesites, dacites, and late Devonian to early Carboniferous metasediments (shale, siltstone, greywacke, sandstone, and limestone). The volcanic rocks formed in an island arc setting, and the metasediments were deposited in a fore-arc basin.

The central unit (terranes 2 and 3) consists predominantly of Neoproterozoic to middle-late Ordovician low-grade sedimentary and volcanic rocks in the northwest

(Shan et al. 2005; Long et al. 2008), and middle-Ordovician to Silurian amphibolite- and greenschist-facies metasediments and metavolcanic rocks in the southwest. Some high-grade metamorphic rocks are thought to be Neoproterozoic in age (e.g., Windley et al. 2002; Li et al. 2003; Xiao et al. 2004), and these rocks were considered to constitute the nuclei of the Altai microcontinent (Hu et al. 2000; Li et al. 2003; Xiao et al. 2004; Wang et al. 2009).

The southern unit is composed of terranes 4 and 5. Terrane 4 can be divided into the Kangbutiebao Formation and the Altai Formation (Windley et al. 2002). The Kangbutiebao Formation consists mainly of arc-type volcanic and pyroclastic rocks, and minor basic volcanics and spilites, and two similar zircon ages of 407 ± 9 Ma (Zhang et al. 2000) and 413 ± 4 Ma (Chai et al. 2008) were obtained from the volcanic rocks. The Altai Formation is made up of low-grade metamorphic rocks, such as a turbiditic sandstone-shale sequence, together with minor basalts, siliceous volcanics, and limestones, which contain middle Devonian fossils. These rocks are interpreted as having been deposited in a fore-arc basin (Windley et al. 2002; Long et al. 2007). Recently, an ophiolite complex was found in the eastern part (Kuerti area) of terrane 4 (Fig. 1) (Xu et al. 2001), and a related plagiogranite yielded a SHRIMP U–Pb zircon age of 372 ± 19 Ma (Zhang et al. 2003). There are also amphibolite-greenschist-facies metasedimentary rocks in terrane 4 (particularly in the southern part), which are considered as pre-Ordovician in age (e.g., Hu et al. 2000; Wang et al. 2006). Terrane 5 contains high-grade gneisses and schists, which formed in the Carboniferous (Liu et al. 2008a), instead of being Precambrian in age as previously suggested (Qu and Chong 1991).

The Erqis (or Irtysh, Ertix, and Erqishi) fault, one of the largest strike-slip faults in Asia, separates the Altai orogen from the Junggar block to the south (Fig. 1). The fault underwent right-lateral movement in the late Carboniferous and early Permian (Tong et al. 2006a; Zhou et al. 2007b; Briggs et al. 2007). Two alkaline granite belts (Bulgen belt and Ulungur belt, <100 km) developed on the northern and southern side of this large fault zone (Fig. 1). U–Pb and Rb–Sr isotopic analyses define ages between 320 and 300 Ma for the Ulungur alkaline plutons (Liu et al. 1996; Han et al. 1997, 2006) and an age of 286 ± 1 Ma for the Takeshiken syenite from the Bulgen belt (Tong et al. 2006b).

The Bulgen granite

The Bulgen alkaline granite crops out in the Erqis fault zone, about 10 km south of the Mongolia–China border (southeast Qinghe country, Xinjiang Uygur Autonomous Region). The Takeshiken syenite is located 12 km SE of the Bulgen pluton (Figs. 1, 2). Country rocks are Proterozoic-Ordovician, Devonian, and Carboniferous strata, chiefly composed of volcanic tuff, breccia, tuffstone, sandstone, andesite, and porphyrite. Mesozoic sediments are very rare, whereas Quaternary deposits cover large areas.

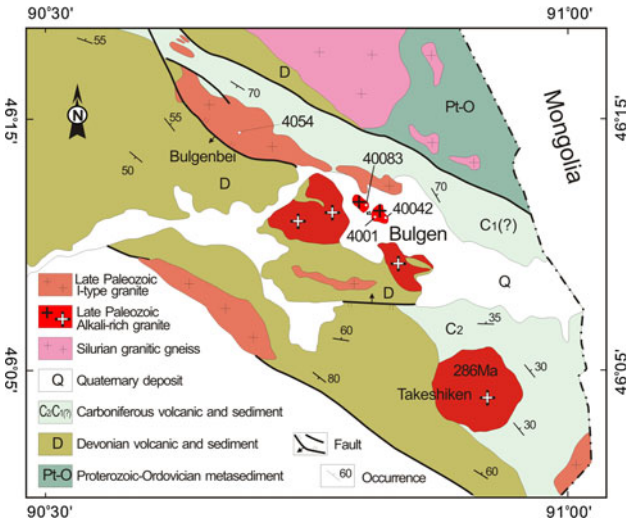

Fig. 2 Geological map of the Bulgen alkaline granite

The Bulgen pluton, the only typical alkaline granite in this region, shows an irregular shape and is virtually undeformed. It covers an area of 1–2 km^2 and consists mainly of medium-grained arfvedsonite alkaline granite. Medium- to fine-grained porphyritic alkaline granites occur in the eastern part of the pluton, whereas fine-grained alkaline granitic dykes with chilled margins can be found in the northern part. These rocks contain up to 30% crystals of arfvedsonite. Analyses were carried out on two arfvedsonite alkaline granites:

Sample 4001 was collected from the eastern part of the Bulgen pluton, E 46°11′08.2″, N 90°48′36.8″. The rock is composed of alkali feldspar (60%), plagioclase (8%), quartz (20%), arfvedsonite (10%), and biotite (<2%). Simultaneous growth of quartz and feldspar has produced a typical graphic texture. Most arfvedsonite crystals are flaky and acicular, show a navy blue color in plain polarized light and are partly replaced by biotite. Alkali feldspars are mainly perthite. Accessory minerals include magnetite, zircon, and sphene. The zircon grains extracted from this sample are colorless or pink, and transparent. Most of them tend to occur as euhedral crystals with short prism faces, usually 100–200 μm along long axis. Concentric oscillatory zoning typical of magmatic origin is developed in all crystals. Few grains have premagmatic domains with rounded cores and oscillatorily zoned rims (e.g., spot 9, Fig. 3).

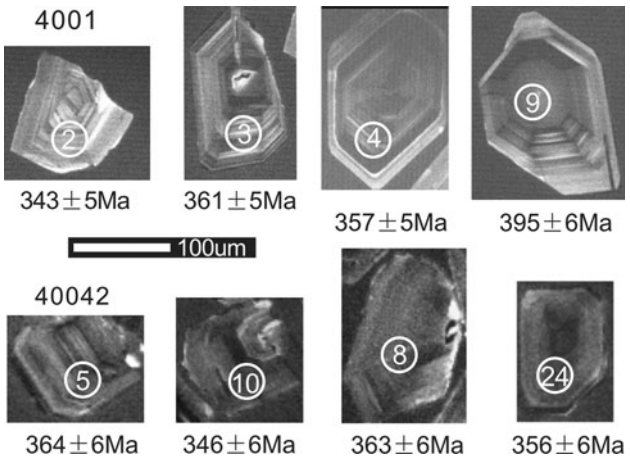

Fig. 3 CL images and U–Pb ages of zircons from the Bulgen alkaline granite

Sample 40042 comes from the eastern part of the pluton, E46°11′21.4″, N 90°48′53.7″. It contains perthite (55%), plagioclase (5%), quartz (25%), arfvedsonite (12%), and biotite (3%). Accessory minerals are sphene, zircon, magnetite, and apatite. Miarolitic textures, presence of alkali feldspar, quartz, and arfvedsonite can be seen under the microscope and bear evidence for magmatic volatile exsolution. The zircons from this sample have similar features as those in sample 4001, and most of them are fine crystals with typical magmatic features that lack inherited cores (Fig. 3).

Analytical methods

U–Pb zircon geochronology

CL imaging of polished zircons embedded in epoxy was conducted on a JEOL scanning electron microscope. Zircon U–Pb dating was performed at the Beijing SHRIMP center of the Chinese Academy of Geological Sciences, using standard operating condition (Williams 1998). U-Th-Pb ratios were determined relative to the TEMORA standard zircon (Black et al. 2003), and the U, Th concentrations were measured relative to SL13. Pb isotope ratios were corrected for common Pb using non-radiogenic ^{204}Pb, and an average crustal composition (Stacey and Kramers 1975) appropriate to the age of the mineral was assumed. U–Pb isotope data were calculated and plotted using the SQUID (1.02) and Isoplot 3.0 (Ludwig 2003) programs. Individual analyses (Table 1) are presented as 1σ error boxes on the concordia diagrams, and age uncertainties are quoted at the 95% confidence level (2σ).

In situ zircon analysis (Laser ablation ICP-MS) was carried out on an Agilent 7500A ICP-MS system, equipped with a GeoLas 200 M (MicroLas, Göttingen, Germany), in the Key Laboratory of Continental Dynamics, Northwest University, Xi'an; the spot size was 30 μm. Zircon 91500 and NIST SRM 610 were used as external standards for the age and concentration calculation, respectively, and ^{29}Si (32.8% SiO_2) was chosen as the internal standardization. Isotope ratios and elemental concentrations were calculated and plotted by using the GLITTER 4.0 software (Macquarie University), and the age calculation was performed with Isoplot 3.0 (Ludwig 2003). For common Pb correction, the software developed by Andersen (2002) was employed.

Major and trace element analysis

Major and trace elements were analyzed at the Key Laboratory of Continental Dynamics of the Northwest University, Xi'an. Major element abundances, except Fe_2O_3 and LOI that were analyzed by wet chemical methods, were determined by X-ray fluorescence (RIX2100X sequential spectrometer). Accuracies of the XRF analyses are greater than 5%. Trace elements and REE were determined by ICPMS (Elan 6100DRC). The analytical accuracies are greater than 5% for Co, Ni, Zn, Ga, Rb, Y, Zr, Nb, Hf, Ta, and LREE and vary between 5 and 15% for other elements.

Sr and Nd isotope compositions

Sr–Nd isotope analyses were conducted on a multicollector VG-354 thermal ionization mass spectrometer at the Isotope Laboratory of the Institute of Geology and Geophysics, Chinese Academy of Sciences, Beijing. The analytical procedures are given in Qiao (1988). Rb, Sr, Sm, and Nd concentrations were determined by the isotope dilution method using a mixed ^{87}Rb-^{84}Sr-^{149}Sm-^{150}Nd spike solution. All measured ^{87}Sr/^{86}Sr and ^{143}Nd/^{144}Nd ratios were normalized to ^{86}Sr/^{88}Sr 0.1194 and ^{146}Nd/^{144}Nd 0.7219, respectively. The La Jolla Nd standard gave a mean ^{143}Nd/^{144}Nd ratio of 0.511863 ± 7 (2σ, $n = 6$). Uncertainties for ^{87}Rb/^{86}Sr are 2% and for ^{147}Sm/^{144}Nd ca. 0.5%. Information on the calculation of εNd, $f_{Sm/Nd}$, and T_{DM}, as well as blank values, analytical precision, and accuracy of the Sr and Nd isotope data, is listed in Table 3.

Results

U–Pb Zircon ages

Ten U–Pb SHRIMP analyses were obtained on zircons from sample 4001 (Table 1; Fig. 4a). The core domain of one zircon gave an old ^{206}Pb/^{238}U age of 395 ± 6 Ma,

Table 1 Zircon U–Pb isotopic analytical data of the Bulgen alkaline granite

Spot	$\%^{206}Pbc$	U ppm	Th ppm	$^{206}Pb^*$ ppm	$^{232}Th/^{238}U$	$^{207}Pb^*/^{206}Pb^*$	± %	$^{207}Pb^*/^{235}U$	± %
Sample 4001, SHRIMP (358 ± 4 Ma)									
4001.1	0.00	359.60	207.10	17.30	0.60	0.0563	5.1	0.4330	5.3
4001.2	0.34	201.15	95.18	9.49	0.49	0.0517	5.1	0.3900	5.3
4001.3	0.00	346.94	296.33	17.20	0.88	0.0556	2.4	0.4420	2.7
4001.4	0.18	692.55	717.40	34.00	1.07	0.0520	2.1	0.4080	2.6
4001.5	0.09	397.25	237.23	19.90	0.62	0.0526	2.5	0.4240	2.9
4001.6	0.35	252.95	115.34	12.60	0.47	0.0487	5.1	0.3870	5.3
4001.7	0.43	234.56	103.13	11.70	0.45	0.0519	4.7	0.4140	5.4
4001.8	0.23	268.49	116.66	13.40	0.45	0.0532	3.3	0.4240	3.7
4001.9*	0.00	338.05	259.23	18.30	0.79	0.0544	4.6	0.4740	4.8
4001.10	0.34	419.17	288.43	20.60	0.71	0.0557	3.7	0.4390	5.9
Sample 40042, LA-ICP-MS (354 ± 4 Ma)									
40042-1	0.51	12.00	47.12	4.15	1.00	0.0536	5.45	0.4075	5.18
40042-2	0.52	85.85	242.15	26.58	0.67	0.0542	1.99	0.4158	1.59
40042-3	0.00	57.16	99.69	16.38	0.40	0.0537	2.01	0.4194	1.60
40042-4	0.29	60.50	112.59	17.35	0.43	0.0532	5.49	0.4067	3.10
40042-5	0.73	91.15	103.47	30.91	0.48	0.0547	3.77	0.4375	3.39
40042-6	0.00	337.39	88.78	109.18	0.42	0.0528	2.01	0.4156	1.61
40042-7	0.04	57.34	121.98	16.66	0.48	0.0546	2.01	0.4085	1.60
40042-8	0.00	113.68	119.59	84.42	0.48	0.0538	2.01	0.4308	1.61
40042-9	0.48	48.31	96.16	110.87	0.48	0.0548	3.69	0.4243	3.30
40042-10	0.15	53.46	103.31	15.52	0.45	0.0539	2.00	0.4104	1.61
40042-11	0.02	49.55	88.74	19.35	0.42	0.0557	2.01	0.4290	1.63
40042-12	0.05	60.55	117.01	52.30	0.45	0.0539	2.00	0.4117	1.63
40042-13	0.00	58.07	141.72	17.38	0.59	0.0535	2.02	0.4142	1.63
40042-14	0.00	68.04	64.82	18.30	0.38	0.0535	1.98	0.4197	1.62

Spot	$^{206}Pb^*/^{238}U$	± %	$^{206}Pb/^{238}U$ (Ma)	$^{207}Pb/^{206}Pb$ (Ma)	$^{208}Pb/^{232}Th$ (Ma)
Sample 4001, SHRIMP (358 ± 4 Ma)					
4001.1	0.0558	1.5	350 ± 5	464 ± 110	342 ± 8.9
4001.2	0.0547	1.6	343 ± 5	273 ± 120	328 ± 16
4001.3	0.0577	1.4	361 ± 5	438 ± 53	364 ± 8.9
4001.4	0.0570	1.4	357 ± 5	285 ± 48	347 ± 6
4001.5	0.0584	1.5	366 ± 5	314 ± 56	366 ± 9.9
4001.6	0.0576	1.4	361 ± 5	132 ± 120	347 ± 16
4001.7	0.0579	2.7	363 ± 10	280 ± 110	337 ± 19
4001.8	0.0578	1.5	362 ± 5	337 ± 75	363 ± 12
4001.9*	0.0632	1.5	395 ± 6	388 ± 100	421 ± 10
4001.10	0.0571	4.6	358 ± 16	442 ± 83	358 ± 25
Sample 40042, LA-ICP-MS (354 ± 4 Ma)					
40042-1	0.0552	1.74	346 ± 6	352 ± 126	358 ± 4
40042-2	0.0557	1.58	349 ± 6	377 ± 16	330 ± 4
40042-3	0.0566	1.59	355 ± 6	358 ± 16	365 ± 4
40042-4	0.0555	1.62	348 ± 6	335 ± 82	364 ± 4
40042-5	0.0581	1.69	364 ± 6	398 ± 86	400 ± 4
40042-6	0.0571	1.58	358 ± 6	318 ± 16	391 ± 4
40042-7	0.0542	1.59	340 ± 6	396 ± 16	341 ± 4

Table 1 continued

Spot	$^{206}Pb^*/^{238}U$	± %	$^{206}Pb/^{238}U$ (Ma)	$^{207}Pb/^{206}Pb$ (Ma)	$^{208}Pb/^{232}Th$ (Ma)
40042-8	0.0580	1.59	363 ± 6	363 ± 16	357 ± 4
40042-9	0.0562	1.64	353 ± 6	402 ± 84	375 ± 4
40042-10	0.0552	1.59	346 ± 6	366 ± 16	338 ± 4
40042-11	0.0558	1.61	350 ± 6	439 ± 16	349 ± 4
40042-12	0.0553	1.63	347 ± 6	368 ± 16	349 ± 4
40042-13	0.0560	1.61	351 ± 6	350 ± 16	330 ± 4
40042-14	0.0567	1.62	356 ± 6	352 ± 16	349 ± 4

Errors are 1σ; Pb_c and Pb* indicate the common and radiogenic portions, respectively; Common Pb was corrected using measured ^{204}Pb

similar to the ages obtained from the widespread early-middle Paleozoic granitic gneisses and gneiss granitoids (Fig. 1); consequently, this zircon domain is interpreted to be inherited. The other nine data points (one spot analysis on a zircon core and eight on rim zones) define a homogeneous age group, yielding a weighted mean $^{206}Pb/^{238}U$ age of 358 ± 4 Ma (MSWD = 0.64). This age is interpreted as the crystallization age of these zircons and thus as the formation age of the pluton.

Zircons from sample 40042 were analyzed by LA-ICP-MS (Table 1; Fig. 4b). Fourteen data points are concordant, yielding a weighted mean $^{206}Pb/^{238}U$ age of 354 ± 4 Ma (MSWD = 0.96), an age indistinguishable from that of sample 4001.

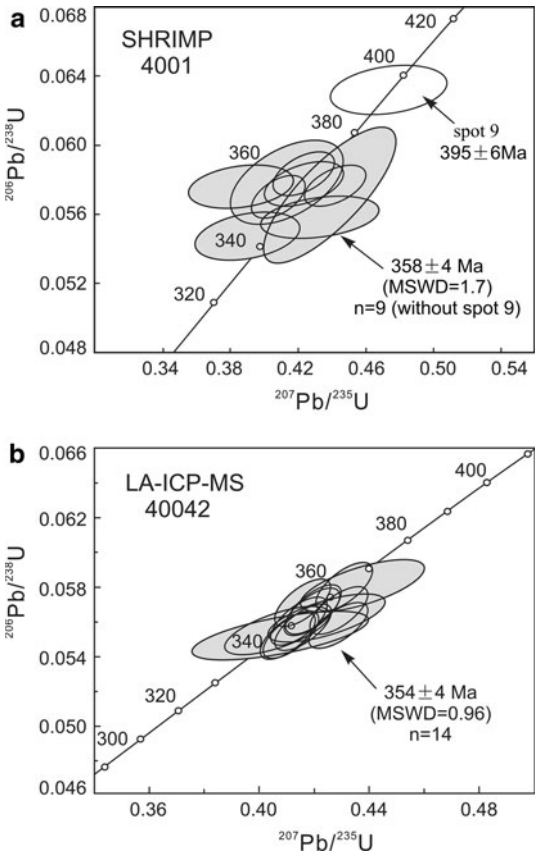

Fig. 4 SHRIMP and LA-ICP-MS U–Pb zircon concordia diagrams for the Bulgen alkaline granite. Error ellipses are 2σ; weighted mean of $^{206}Pb/^{238}U$ ages are reported, with data marked by white ellipse excluded from weighted mean calculation

Geochemical and Sr–Nd isotope composition

Our new data and other data from Zhao et al. (1993) and Liu et al. (1996) show that the rocks of the Bulgen pluton are enriched in silica (SiO_2 from 71.5 to 77.1%), total alkalis ($Na_2O + K_2O$ = 8.56–10.62%), and Fe* [FeOt/(FeOt + MgO) = 0.88–0.98] (Table 2). Except sample k-1-3 (porphyritic alkaline granite), all other samples are mildly metaluminous to peralkaline, with A/CNK (molar ratio of $Al_2O_3/[CaO + Na_2O + K_2O]$) and A/NK (molar ratio of $Al_2O_3/[Na_2O + K_2O]$) ratios generally ranging from 0.87 to 1.02 and 0.81 to 1.02, respectively. The samples have low abundances of Al_2O_3 (11.73–12.67%), MnO (0.03–0.11%), P_2O_5 (≤0.06%), and TiO_2 (0.08–0.37%) (Table 2).

The Bulgen granite is highly enriched in rare earth elements (REE), with total REE = 185–509 ppm. In a chondrite-normalized REE diagram, samples show uniform compositions with light REE enrichment, pronounced negative Eu anomalies (Eu/Eu* = 0.02–0.20), La_N/Yb_N ratios of 2.9–7.1, and flat heavy REE pattern (Fig. 5a). In normalized trace element diagrams (Fig. 5b), all rocks have high concentrations of high-field-strength elements (HFSE, Th, Zr, Hf, Nb, and Ce) and show negative anomalies in Ba, Sr, P, and Ti. 10000*Ga/Al ratios range from 2.7 to 4.9. All these geochemical characteristics are also observed in typical alkaline (A-type) granites (Whalen et al. 1987).

Sr and Nd isotope data of this study, together with literature data, are given in Table 3. The Bulgen alkaline granite has high $^{143}Nd/^{144}Nd$ ratios (0.51277–0.51290).

Table 2 Chemical composition of the Bulgen alkaline granite (major elements in wt%, trace elements in ppm)

Rock	Alkaline granite										PA granite
Sample no.	4001	40083	4042	N5-3*	k-1-2*	k-1-10*	kou-3*	8746*	8753*	8725*	k-1-3*
SiO_2	73.14	74.77	77.07	73.02	73.16	74.64	76.17	71.46	74.27	75.25	76.30
TiO_2	0.20	0.20	0.08	0.19	0.23	0.20	0.14	0.37	0.22	0.17	0.11
Al_2O_3	12.67	11.81	11.89	12.47	12.62	12.04	12.03	11.73	11.90	11.89	12.32
Fe_2O_3	1.14	1.92	0.71	1.08	1.60	1.67	0.72	1.84	2.51	1.17	1.07
FeO	1.49	0.97	0.79	1.53	1.71	1.15	1.11	1.51	0.76	1.04	0.58
MnO	0.11	0.09	0.04	0.09	0.10	0.03	0.04	0.13	0.13	0.07	0.02
MgO	0.07	0.10	0.10	0.34	0.09	0.09	0.10	0.20	0.05	0.05	0.08
CaO	0.42	0.40	0.29	0.69	0.62	0.87	0.97	0.91	0.54	0.92	0.28
Na_2O	4.76	4.30	4.59	4.62	4.77	4.26	4.09	5.23	4.09	4.15	3.91
K_2O	5.13	4.96	4.54	5.06	4.57	4.68	4.69	5.39	5.00	4.41	4.70
P_2O_5	0.01	0.01	0.01	0.03	0.06	0.02	0.02				0.02
H_2O	0.40	0.24	0.34	0.19	0.36	0.28	0.08				0.16
LOI	0.28	0.32	0.26								
Total	99.82	100.09	100.71	99.31	99.89	99.93	100.16	98.77	99.47	99.12	99.55
NK/A	1.06	0.95	0.95	0.95	0.99	1.00	1.02	0.81	0.98	1.02	1.07
FeOt	2.52	2.70	1.43	2.50	3.15	2.65	1.76	3.17	3.02	2.09	1.54
Rb	219	180	216	200	230	219	250				130
Sr	19.3	13.4	6.3	14.0	14.7	12.8	10.0				20.0
Ba	18.3	19.3	7.3	21.0	23.7	24.2	21.0				20.0
Nb	89	104	91	69	122	91	70				48
Ta	7.2	7.6	7.6	1.1	1.4	1.3	0.1				0.6
Th	19.5	20.1	24.7		19.2	18.1					
U	3.3	2.6	6.4								
Zr	783	921	438	365	1321	1047	274				272
Hf	22.4	27.5	15.5								
Ga	32	30	32	33	25	23	26				21
Zn	179	144	96	98	126	94	77				26
Y	60	91	87	78	111	88	81	39	43	42	48
La	72	109	52	60	61	58	64	48	49	57	50
Ce	139	213	103	122	156	133	127	89	105	114	93
Pr	16.4	22.8	12.3	16.0	12.9	13.6	17.7	11.7	12.8	13.8	12.9
Nd	56	81	45	51	48	42	53	39	43	45	40
Sm	12.4	16.9	12.6	10.9	12.6	0.9	12.1	7.4	7.9	8.7	8.0
Eu	0.19	0.26	0.14	0.20	0.86	1.81	0.27	0.79	0.24	0.66	0.08
Gd	9.6	13.6	12.2	10.2	10.9	9.9	10.9	8.7	9.3	10.7	6.6
Tb	2.0	2.8	2.7	1.8	2.1	1.9	1.9	1.5	1.4	1.7	1.5
Dy	12.6	17.3	17.9	13.3	13.5	13.0	13.2	7.8	8.2	8.9	8.2
Ho	2.8	3.7	4.0	2.7	3.3	2.9	2.7	1.7	1.7	2.0	1.7
Er	8.8	12.0	12.2	8.8	9.8	7.8	8.3	4.7	5.2	5.2	5.5
Tm	1.5	1.9	2.0	1.4	1.8	1.4	1.3	0.8	0.7	0.7	0.9
Yb	10.4	13.0	12.9	10.0	13.2	10.9	9.3	5.3	6.0	5.8	6.5
Lu	1.8	2.0	2.0	1.6	2.0	1.7	1.4	1.0	1.0	1.1	1.0
REE	346	509	291	310	348	298	323	185	185	319	237

PA porphyritic alkaline

NK/A = $(Na_2O + K_2O)/Al_2O_3$, mol%; FeOt = FeO + (Fe2O3 * 0.8998)

* Data from Zhao et al. (1993) and Liu et al. (1996)

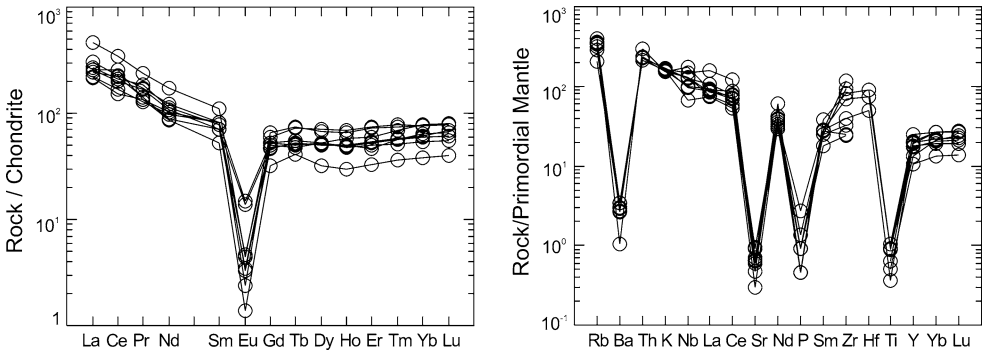

Fig. 5 Chondrite-normalized REE patterns and primitive mantle-normalized spidergrams for the Bulgen alkaline granite. Common features of all samples are the negative anomalies in Eu, Ba, Sr, P, and Ti. The chondrite values and values of primitive mantle are from Sun and McDonough (1989)

The εNd(t) value vary from +6.3 to +6.4, and the Nd model ages (T_{DM}) are between 460 and 773 Ma.

Discussion

The pluton formation age

Wang et al. (1998) reported a whole-rock and mineral Rb–Sr age of 253 ± 13 Ma for the Bulgen alkaline granite. Liu et al. (1996) obtained an apparently old whole-rock Rb–Sr age of 301 Ma. They argued that the alkaline granite must be younger than the alkali-feldspar granite for which they obtained a U–Pb zircon age of 287 Ma. The two samples analyzed in this study yield nearly the same U–Pb ages (358 ± 4 Ma, 354 ± 4 Ma), and the ages of mantle, core, and rim domains of various grains are almost identical. Based on these results, we propose that the Bulgen pluton formed during the early Carboniferous.

Petrogenesis of the Bulgen alkaline granite

A-type granites play a critical role in granite petrology, but there is still no consensus on their exact formation. Current petrogenetic models on the origin of these rocks include fractional crystallization of alkaline basaltic magma (Loiselle and Wones 1979; Turner et al. 1992) or partial melting of relatively refractory granulitic (Collins et al. 1982; Whalen et al. 1987), tonalitic (Creaser et al. 1991) or alkali-metasomatized (Martin 2006) lower crustal compositions. It was also reported that some A-type granites have geochemical characteristics of magma derived from an oceanic island basalt (OIB)-type source (Eby 1990, 1992).

The Bulgen alkaline granite has high LILE and HFSE abundances, which could be explained by an OIB-like component in the magma source. The pronounced negative Eu anomaly indicates the importance of plagioclase fractionation contemporaneous with crystallization or, alternatively, it would require plagioclase in the residue in case of an anatectic origin (Cullers and Graf 1984). The lack of negative Nb anomaly seen in all samples suggest that the granite melts did not originate by partially melting a (supra) subduction zone environment.

The εNd(*t*) values of the Bulgen alkaline granite range from +6.3 to +6.4 and are higher than those of the early-middle Paleozoic granitoids (−2.6 to +4.2, Wang et al. 2006), but similar to those of the Ulungur alkaline granitoids (+5.5 to +6.7, Han et al. 1997) and the Takeshiken syenite (+6.2 to +6.3, Tong et al. 2006b) (Fig. 6). The positive εNd(*t*) values for Bulgen granite thus suggest the addition of juvenile mantle-derived material with negligible involvement of older crust as opposed to the other early-middle Paleozoic granitoids, which show a clear crustal signature.

Tectonic implications

Although some authors argued that A-type granites can form in back-arc or intra-arc settings (Zhao et al. 2008), it is commonly accepted that A-type granites form in post-collision to post-orogenic settings, and continental or oceanic intra-plate settings (Bonin 1990, 2007; Eby 1992; Hong et al. 1996 and references therein).

The Bulgen pluton (358–354 Ma), clearly postdating the syn-orogenic granitoids (460–375 Ma), sheds light on late Paleozoic orogenic process in the Chinese Altai. From the early-middle Paleozoic to the late Paleozoic, magmatism in this region evolved progressively from mostly I-type tholeiitic to calc-alkaline igneous activity (Wang et al. 2006; Zhang et al. 2006) to A-type alkaline granite such as the Bulgen granite. The A-type granites are characterized by high Rb, Nb, and Y contents, unlike arc granites and ocean-ridge granites. The Bulgen pluton is undeformed and irregular in shape. It is intruded by fine-grained alkaline granitic dykes, which show typical miarolitic and micrographic textures. In contrast, the early-middle Paleozoic granitoids plutons occur as elongated deformed bodies, parallel to the prevailing tectonic fabric of the host rocks.

Table 3 Sr–Nd isotope data of the granites from the Bulgen area

Sample no.	Rock	Locality (Pluton name)	Age (Ma)	Rb	Sr	$^{87}Rb/^{86}Sr$	$^{87}Sr/^{86}Sr$	2σ	I_{Sr}	Sm	Nd
Early carboniferous											
40042	Alkline granite	Bulgen	358	251.32	10.24	40.018	0.898289	18	0.6943	10.69	38.35
40083	Alkline granite	Bulgen	358	245.40	15.03	48.790	0.922620	20	0.6740	17.46	92.09
BG-6	Alkali-spar granite	Bulgennan	358	225.14	56.12	11.610	0.756290	9	0.6971	6.46	30.37
BG-0	Granodiorite	Bulgennan	358	86.20	700.90	0.350	0.705460	22	0.7037	3.93	19.54
4054	Biotite monzogranite	Bulgenbei	343	68.21	585.60	0.340	0.705380	10	0.7037	3.36	17.37
Permian											
380105	Synite	Takeshiken	286	46.79	298.0	0.450	0.705850	10	0.7040	8.72	43.93
380101-2	Syenogranite	Takeshiken	286	91.80	122.10	2.180	0.712660	11	0.7038	7.76	40.38
380102-1	Mafic dyke	Takeshiken	286	8.17	532.4	0.040	0.704660	10	0.7045	2.24	8.18

Sample no.	Rock	Locality (Pluton name)	$^{147}Sm/^{144}Nd$	$^{143}Nd/^{144}Nd$	2σ	$\varepsilon Nd\ (0)$	f (Sm/Nd)	$\varepsilon Nd\ (t)$	T_{DM}-1 (Ma)	T_{DM}-2 (Ma)	Data source
Early carboniferous											
40042	Alkline granite	Bulgen	0.1688	0.512897	13	5.2	−0.14	6.5	859	590	This study
40083	Alkline granite	Bulgen	0.1148	0.512771	12	2.8	−0.41	6.5	585	592	This study
BG-6	Alkali-spar granite	Bulgennan	0.1287	0.512736		2.1	−0.34	5.2	743	698	Zhao et al. (1993)
BG-0	Granodiorite	Bulgennan	0.1216	0.512672		0.8	−0.38	4.2	792	773	Zhao et al. (1993)
4054	Biotite monzogranite	Bulgenbei	0.1171	0.512789	11	3.1	−0.40	6.6	570	572	This study
Permian											
380105	Synite	Takeshiken	0.1200	0.512816	10	3.6	−0.39	6.4	544	538	Tong et al. (2006b)
380101-2	Syenogranite	Takeshiken	0.1162	0.512805	11	3.4	−0.41	6.3	540	544	Tong et al. (2006b)
380102-1	Mafic dyke	Takeshiken	0.1656	0.512949	10	6.2	−0.16	7.3	638	460	Tong et al. (2006b)

$\varepsilon_{Nd} = (((^{143}Nd/^{144}Nd)_s/(^{143}Nd/^{144}Nd)_{CHUR} - 1) \times 10{,}000$, $f_{Sm/Nd} = (^{147}Sm/^{144}Nd)_s/(^{147}Sm/^{144}Nd)_{CHUR} - 1$, where s = sample, $(^{143}Nd/^{144}Nd)_{CHUR} = 0.512630$, and $(^{147}Sm/^{144}Nd)_{CHUR} = 0.1960$ (Bouvier et al. 2008). The model ages (T_{DM}) were calculated using a linear isotopic ratio growth equation, $T_{DM} = 1/\lambda x\ \ln(1 + ((^{143}Nd/^{144}Nd)_s - 0.51315)/((^{147}Sm/^{144}Nd)_s - 0.2137))$. The two-stage model age is obtained assuming that the protolith of the granitic magmas has a Sm/Nd ratio (or $f_{Sm/Nd}$ value) of the average continental crust (Keto and Jacobsen 1987). The T_{DM}-2 = (T_{DM}1-(T_{DM} 1 − t)(fcc-fdm))/(fcc-fdm), where fcc, fs, and fdm = $f_{sm/Nd}$ values of the average continental crust, the sample and the depleted mantle, respectively. fcc = 0.4, fdm = 0.08592, and t = the intrusive age of granite

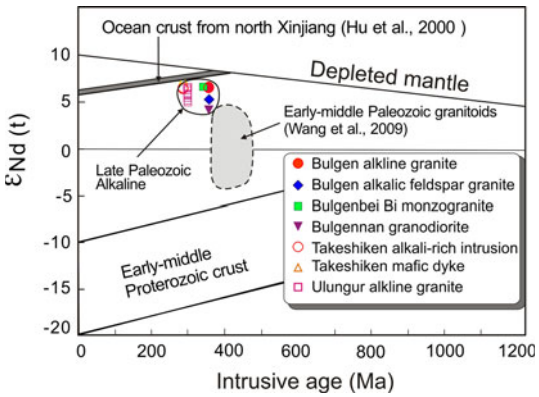

Fig. 6 εNd(t) versus age (Ma) diagram for granitoids from the Chinese Altai. Note that the εNd(t) values of the granites increase from early-middle Paleozoic to late Paleozoic (data from Table 3)

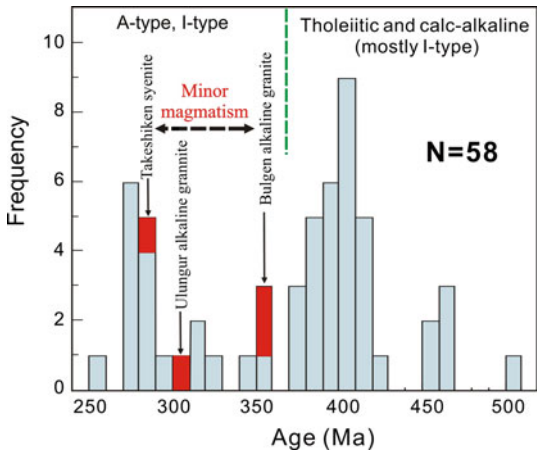

Fig. 7 Age histogram of the Chinese Altai granitoids (same data as in Fig. 1). Alkaline granitoids shown by *red bar*

These variations, together with the progressive change in εNd values toward mantle values (see above), indicate that the tectonic regime significantly changed from a syn-orogenic regional compression setting to a post-orogenic extensional setting. This, in turn, suggests that the main orogenic processes in the Chinese Altai ceased after the early Carboniferous.

This conclusion is also supported by regional geological evidence. The folded early Carboniferous "Nanmingshui" Formation in this area was intruded by the undeformed Bulgenbei biotite monzogranite at about 343 ± 3 Ma (authors unpublished data) demonstrating that the formation and deformation of these rocks occurred prior to this age. The late Carboniferous volcano-sedimentary stratum formed in a typical continental volcano-sediment system (Zhang et al. 2007). No major magmatism occurred from 350 to 280 Ma (Fig. 7), and there is no evidence for regional metamorphism and deformation during this

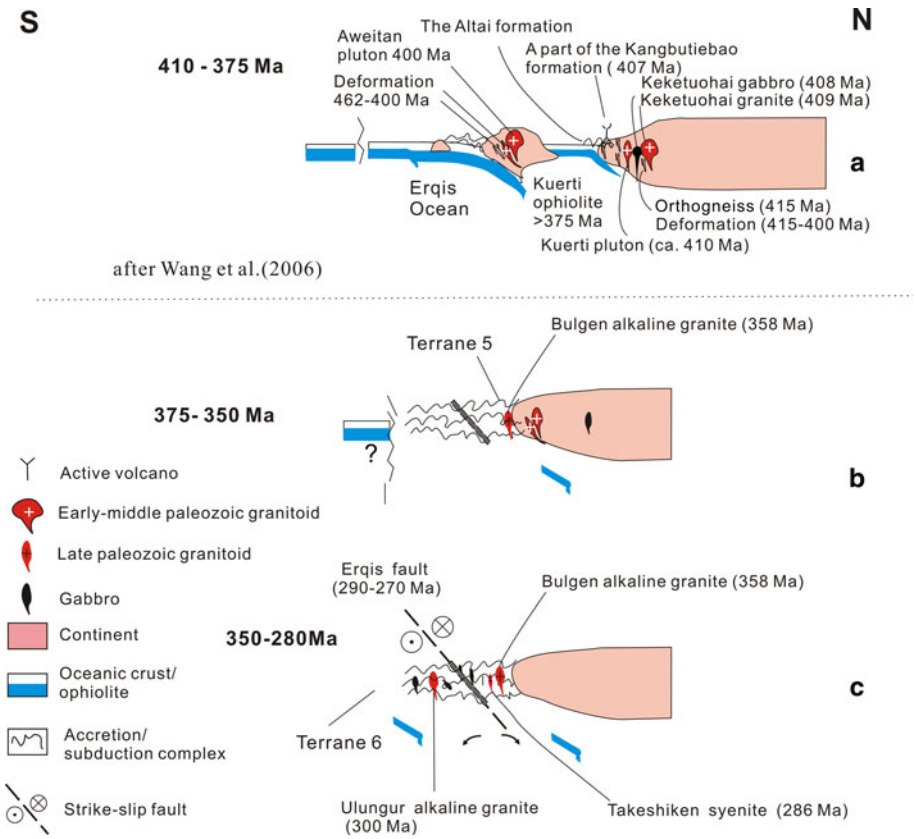

Fig. 8 Tectonic model showing the middle- and late-Paleozoic evolution of the Chinese Altai (Fig. 8a after Wang et al. 2006)

period. Actually, all metamorphosed or deformed rocks are restricted to the narrow Erqis fault zone, which underwent right-lateral movement after 290 Ma (Tong et al. 2006a; Zhou et al. 2007b; Briggs et al. 2007; Sun et al. 2009b). The ophiolites in the Altai orogen and adjacent regions formed approximately between 500 and 375 Ma (Li 1995; Jian et al. 2003; Zhang et al. 2003; Xiao et al. 2004), and no 350–250 Ma old ophiolites have been reported so far, which would not give evidence for formation of new oceanic crust during this period. All these observations support the view that the Altai orogeny ended during the late Paleozoic causing a complete consumption of the Erqis Ocean (Fig. 8).

Generally, successive accretion of arc crust or a collage of terranes is emphasized as a major process in the formation of the Altaids collage or CAOB (e.g., Coleman 1989; Sengör et al. 1993; Windley et al. 2002; Badarch et al. 2002; Xiao et al. 2004). The magmatic cycles in the Altai orogen might have been associated with similar tectonic cycles. This is consistent with the observation that the Altai orogen underwent a series of processes involving the formation of an active continental margin, the break-up of this margin to form a back-arc ocean, and the final closure of the back-arc ocean. Such a tectonic scenario is probably very common in other accretionary orogens (Wang et al. 2006). This gives rise to the final hypothesis that the evolution and the long-lived accretionary history of the CAOB were dominated by a periodic component of synchronous magmatic and tectonic cycles.

Conclusions

U–Pb dating of zircons with SHRIMP and LA-ICP-MS shows that the Bulgen alkaline granite formed in the early Carboniferous (about 358–354 m.y.a.). All geochemical data indicate that partial melting of juvenile mantle-derived material in an extensional post-orogenic setting generated the pluton. Emplacement of the granite took place at least 15 Ma after the formation of the syn-orogenic granitoids (460–375 Ma). The occurrence of young post-orogenic A-type granites implies that the tectonic regime of the Chinese Altai orogen significantly changed from early–middle Paleozoic syn-orogenic regional compression into a late Paleozoic post-orogenic extensional setting during late Devonian to early Carboniferous times.

Acknowledgments We sincerely thank Tom Andersen, Bor-Ming Jahn, E. Hegner, G.C. Zhao, and H.F. Zhang for their constructive and helpful comments. This research was financially supported by the National Natural Science Foundation of China (NSFC grant 40702010), the Chinese National 973 Program (2007CB411307), the Basic Outlay of Scientific Research Work from the Ministry of Science and Technology of the People's Republic of China (J0709, J0906) and the China Geological Survey Project (1212010611803, 1212010611817). We also thank Z.Q. Yan, H. Zhou, and X.M. Liu for laboratory assistance.

References

Andersen T (2002) Correction of common lead in U–Pb analyses that do not report 204Pb. Chem Geol 192(1–2):59–79. doi:10.1016/S0009-2541(02)00195-X

Badarch G, Cunningham WD, Windley BF (2002) A new terrane subdivision for Mongolia: implications for the Phanerozoic crustal growth of Central Asia. J Asian Earth Sci 21(1):87–110. doi:10.1016/S1367-9120(02)00017-2

Black LP, Kamo SL, Williams IS, Mundil R, Davis DW, Korsch RJ, Foudoulis C (2003) The application of SHRIMP to Phanerozoic geochronology; a critical appraisal of four zircon standards. Chem Geol 200(1–2):171–188. doi:10.1016/S0009-2541(03)00166-9

Bonin B (1990) From orogenic to anorogenic settings: evolution of granitoid suites after a major orogenesis. Geol J 25(3–4):261–270. doi:10.1002/gj.3350250309

Bonin B (2007) A-type granites and related rocks: evolution of a concept, problems and prospects. Lithos 97(1–2):1–29. doi:10.1016/j.lithos.2006.12.007

Bouvier A, Vervoort JD, Patchett PJ (2008) The Lu–Hf and Sm–Nd isotopic composition of CHUR: constraints from unequilibrated chondrites and implications for the bulk composition of terrestrial planets. Earth Planet Sci Lett 273(1–2):48–57. doi:10.1016/j.epsl.2008.06.010

Briggs SM, Yin A, Manning CE, Chen ZL, Wang XF, Grove M (2007) Late Paleozoic tectonic history of the Ertix Fault in the Chinese Altai and its implications for the development of the Central Asian Orogenic System. Geol Soc Am Bull 119(7–8):944–960. doi:10.1130/B26044.1

Cai KD, Yuan C, Sun M, Xiao WJ, Chen HL, Long XP, Zhao YJ, Li JL (2007) Geochemical characteristics and ^{40}Ar-^{39}Ar ages of the amphibolites and gabbros in Tarlang area: implications for tectonic evolution of the Chinese Altai. Acta Petrologica Sinica 23(5):877–888 (Chinese with English abstract)

Chai FM, Mao JW, Dong LH, Yang FQ, Liu F, Geng XX, Yang ZX, Huang CK (2008) SHRIMP zircon U–Pb dating for metarhyolites of the Kangbutiebao formation at the Abagong iron deposit in the southern margin of the Altay, Xinjiang and its geological significance. Acta Geol Sinica 82(11):1592–1601 (Chinese with English abstract)

Chen HL, Yang SF, Li ZL, Yu X, Xiao WJ, Yuan C, Lin XB, Li JL (2006) Zircon SHRIMP U–Pb chronology of Fuyun basic granulite and its tectonic significance in Altaid orogenic belt. Acta Petrologica Sinica 22(5):1351–1358 (Chinese with English abstract)

Coleman RG (1989) Continental growth of northwest China. Tectonics 8(3):621–635. doi:10.1029/TC008i003p00621

Collins WJ, Beams SD, White AJR, Chappell BW (1982) Nature and origin of A-type granites with particular reference to southeastern Australia. Contrib Mineral Petrol 80(2):189–200. doi:10.1007/BF00374895

Creaser RA, Price RC, Wormald RJ (1991) A-type granites revisited: assessment of a residual-source model. Geology 19(2):163–166. doi:10.1130/0091-7613(1991)019<0163:ATGRAO>2.3.CO;2

Cullers R, Graf JL (1984) Rare earth elements in igneous rocks of the continental crust: intermediate and silicic rocks-ore petrogenesis. Elsevier, Amsterdam, pp 275–316

Eby GN (1990) The A-type granitoids: a review of their occurrence and chemical characteristics and speculations on their

petrogenesis. Lithos 26(1–2):115–134. doi:10.1016/0024-4937(90)90043-Z

Eby GN (1992) Chemical subdivision of the A-type granitoids: petrogenetic and tectonic implications. Geology 20(4):641–644. doi:10.1130/0091-7613(1992)020<0641:CSOTAT>2.3.CO;2

Han BF, Wang SG, Jahn BM, Hong DW, Kagami H, Sun YL (1997) Depleted-mantle source for the Ulungur River A-type granites from North Xinjiang, China: geochemistry and Nd–Sr isotopic evidence, and implications for Phanerozoic crustal growth. Chem Geol 138(3–4):135–159. doi:10.1016/S0009-2541(97)00003-X

Han BF, Ji JQ, Song B, Chen LH, Zhang L (2006) Late Paleozoic vertical growth of continental crust around the Junggar Basin, Xinjiang, China (part I): timing of post-collisional plutonism. Acta Petrologica Sinica 22(5):1077–1086 (Chinese with English abstract)

He GQ, Han BF, Yue YJ, Wang JH (1990) Tectonic division and crustal evolution of Altay Orogenic Belt in China. Geoscience (Xinjiang) 2:9–20 (Chinese with English abstract)

He GQ, Li MS, Liu DQ, Zhou NH (1994) Palaeozoic crustal evolution and mineralization in Xinjiang of China, Xinjiang, vol 1. People's Publish House, Urumqi, p 437 (Chinese with English abstract)

Hong DW, Wang SG, Han BF, Jin MY (1996) Post-orogenic alkaline granites from China and comparisons with anorogenic alkaline granites elsewhere. J Southeast Asian Earth Sci 30(1):13–27. doi:10.1016/0743-9547(96)00002-5

Hong DW, Zhang JS, Wang T, Wang SG, Xie XL (2004) Continental crustal growth and the super continental cycle: evidence from the Central Asian Orogenic Belt. J Asian Earth Sci 23(5):799–813. doi:10.1016/S1367-9120(03)00134-2

Hu AQ, Jahn BM, Zhang GX, Chen YB, Zhang QF (2000) Crustal evolution and Phanerozoic crustal growth in northern Xinjiang: Nd isotopic evidence, part I. Isotopic characteristics of basement rocks. Tectonophysics 328(1–2):15–51. doi:10.1016/S0040-1951(00)00176-1

Hu AQ, Wei GJ, Deng WF, Chen LL (2006) SHRIMP zircon U–Pb dating and its significance for gneisses from the southwest area to Qinghe County in the Altai, China. Acta Petrologica Sinica 22(1):1–10 (Chinese with English abstract)

Jahn BM (2004) The central Asian orogenic belt and growth of the continental crust in the Phanerozoic. Geol Soc Lond Spec Pub 226:73–100. doi:10.1144/GSL.SP.2004.226.01.05

Jahn BM, Wu FY, Chen B (2000) Granitoids of the central Asian orogenic belt and continental growth in the Phanerozoic. Geol Soc Am Spec Papers 350:181–193. doi:10.1130/0-8137-2350-7.181

Jian P, Liu DY, Zhang Q, Zhang FQ, Shi YR, Shi GH, Zhang LQ, Tao H (2003) SHRIMP dating of ophiolite and leucocratic rocks within ophiolite. Earth Sci Front 10(4):439–456 (Chinese with English abstract)

Keto LS, Jacobsen SB (1987) Nd and Sr isotopic variations of early Palaeozoic oceans. Earth Planet Sci Lett 84(1):27–41. doi:10.1016/0012-821X(87)90173-7

Khain EV, Bibokova EV, Kröner A, Zhuravlev DZ, Sklyarov EV, Fedotova AA, Kravchenko-Berezhnoy IR (2002) The most ancient ophiolites of the central Asian fold belt: U–Pb and Pb–Pb zircon ages for the Dunzhugur complex, Eastern Sayan, Siberia, and geodynamic implications. Earth Planet Sci Lett 199(3–4):311–325. doi:10.1016/S0012-821X(02)00587-3

Kovalenko VI, Yarmolyuk VV, Kovach VP, Kotov AB, Kozakov IK, Salnikova EB, Larin AM (2004) Isotope provinces, mechanisms of generation and sources of the continental crust in the central Asian mobile belt: geological and isotopic evidence. J Asian Earth Sci 23(5):605–627. doi:10.1016/S1367-9120(03)00130-5

Li JY (1995) Main characteristics and emplacement processes of the East Junggar ophiolites, Xinjiang China. Acta Petrologica Sinica 11:73–84 (Chinese with English abstract)

Li JY, Xiao WJ, Wang KZ, Sun GH, Gao LM (2003) Neoproterozoic-Palaeozoic tectonostratigraphy, magmatic activities and tectonic evolution of eastern Xinjiang, NW China. In: Mao J, Goldfarb RJ, Seltman R, Wang W, Xiao D, Hart CJ (eds) Tectonic evolution and metallogeny of the Chinese Altay and Tianshan. IAGOD Guidebook Series 10, CERCAM/NHM, London, pp 31–74

Li ZH, Han BF, Song B (2004) SHRIMP zircon U–Pb dating of the Ertaibei granodiorite and its enclave from eastern Junggar, Xinjiang, and geological implications. Acta Petrologica Sinica 20(5):1263–1270 (Chinese with English abstract)

Liu JY, Yuan KR, Wu GQ (1996) Alkaline granites in Junggar, Xinjiang and their metallization. Central South University of Technology Press, Changsha, pp 13–170 (Chinese with English abstract)

Liu F, Li YH, Mao JW, Yang FQ, Chai FM, Geng XX, Yang ZX (2008a) SHRIMP U–Pb Ages of the Abagong granites in the Altay orogen and their geological implications. Acta Geoscientica Sinica 29(6):795–804 (Chinese with English abstract)

Liu GR, Qin H, Zhao H, Xue HM, Zhang LW, He LX (2008b) SHRIMP U–Pb ages of zircon in the gneiss of Erqisi tectonic belt in Altay, Xinjiang and their geological significances. Geoscience 22(2):190–196 (Chinese with English abstract)

Loiselle MC, Wones DR (1979) Characteristics and origin of anorogenic granites. Abstracts of papers to be presented at the annual meetings of the Geological Society of America, San Diego 11:468

Long XP, Sun M, Yuan C, Xiao WJ, Chen HL, Zhao YJ, Cai KD, Li JL (2006) Genesis of Carboniferous volcanic rocks in the eastern Junggar: constraints on the closure of the Junggar Ocean. Acta Petrologica Sinica 22(1):31–40 (Chinese with English abstract)

Long XP, Sun M, Yuan C, Xiao WJ, Lin SF, Wu FY, Xia XP, Cai KD (2007) Detrital zircon age and Hf isotopic studies for meta sedimentary rocks from the Chinese Altai: Implications for the Early Paleozoic tectonic evolution of the Central Asian Orogenic Belt. Tectonics 26:TC5015. doi:101029/2007TC002128

Long XP, Sun M, Yuan C, Xiao WJ, Cai KD (2008) Early Paleozoic sedimentary record of the Chinese Altai: implications for its tectonic evolution. Sed Geol 208:88–100. doi:10.1016/j.sedgeo.2008.05.002

Long XP, Yuan C, Sun M, Xiao WJ, Zhao GC, Wang YJ, Cai KD, Xia XP, Xie LW (2010) Detrital zircon ages and Hf isotopes of the early Paleozoic flysch sequence in the Chinese Altai, NW China: new constrains on depositional age, provenance and tectonic evolution. Tectonophysics 480(1–4):213–231. doi:10.1016/j.tecto.2009.10.013

Lou FS (1997) Characteristics of late Caledonian granites in the Nuoerte area, Altay. Jiangxi Geol 11(3):60–66 (Chinese with English abstract)

Ludwig KR (2003) A geochronological toolkit for Microsoft Excel. Berkeley Geochronol Center Spec Pub 4:25–32

Mao JW, Franco P, Zhang ZH, Chai FM, Yang JM, Wu H, Chen SP, Cheng SL, Zhang CQ (2006) Late Variscan post-collisional Cu-Ni sulfide deposits in east Tianshan and Altay in China: Principal characteristics and possible relationship with mantle plume. Acta Geol Sinica 80(7): 925–942 (Chinese with English abstract)

Martin RF (2006) A-type granites of crustal origin ultimately result from open-system fenitization-type reactions in an extensional environment. Lithos 91(1–4):125–136. doi:10.1016/j.lithos.2006.03.012

Mossakovsky AA, Ruzhentsev SV, Samygin SG, Kheraskova TN (1993) Central Asian fold belt: geodynamic evolution and history of formation. Geotectonics 6:3–33

Qiao GS (1988) Normalization of isotopic dilution analyses- a new program for isotope mass spectrometric analysis. Scientia Sinica (Series A) 31(10):1263–1268

Qu GS, Chong MY (1991) Lead isotope geology and its tectonic implications in Altaides, China. Geoscience 5(1):100–110 (Chinese with English abstract)

Sengör AMC, Natal'in BA, Burtman VS (1993) Evolution of Altaid tectonic collage and Paleozoic crustal growth in Eurasia. Nature 364:299–307. doi:10.1038/364299a0

Shan Q, Niu HC, Yu XY, Zhang HX (2005) Geochemistry and zircon U–Pb age of volcanic rocks from the Hanasi basin in the northern Xinjiang and their tectonic significance. Geochimica 34(4):315–327 (Chinese with English abstract)

Stacey JS, Kramers JD (1975) Approximation of terrestrial lead isotope evolution by a two-stage model. Earth Planet Sci Lett 26(2):207–221. doi:10.1016/0012-821X(75)90088-6

Sun SS, McDonough WF (1989) Chemical and isotopic systematics of oceanic basalts: implications for mantle compositions and processes. Geol Soc Lond Spec Pub 42:313–345. doi:10.1144/GSL.SP.1989.042.01.19

Sun M, Yuan C, Xiao WJ, Long XP, Xiao XP, Zhao GC, Lin SF, Wu FY, Kröner A (2008) Zircon U–Pb and Hf isotopic study of gneissic rocks from the Chinese Altai: progressive accretionary history in the early to middle Palaeozoic. Chem Geol 247(3–4):352–383. doi:10.1016/j.chemgeo.2007.10.026

Sun M, Long XP, Cai KD, Jian YD, Wang BY, Yuan C (2009a) Early Paleozoic ridge subduction in the Chinese Altai: insight from the abrupt change in zircon Hf isotopic compositions. Science in China 52(9):1345–1358

Sun GH, Li JY, Yang TN, Li YP, Zhu ZX, Yang ZQ (2009b) Zircon SHRIMP U–Pb dating of two linear granite plutons in southern Altay Mountains and its tectonic implications. Geol China 36(5):976–987 (Chinese with English abstract)

Tong Y, Wang T, Hong DW (2005) Zircon U–Pb age of syn-orogenic Tielieke pluton in the western part of Altay orogenic belt and its structural implications. Acta Geoscientica Sinica 26(z1):74–77 (Chinese with English abstract)

Tong Y, Hong DW, Wang T, Wang SG, Han BF (2006a) TIMS U-Pb zircon ages of Fuyun post-orogenic linear granite plutons on the southern margin of Altay orogenic belt and their implications. Acta Petrologica Et Mineralogica 25(2):85–89 (Chinese with English abstract)

Tong Y, Wang T, Kovach VP, Hong DW, Han BF (2006b) Age and origin of the Takeshiken postorogenic alkali-rich intrusive rocks in southern Altai, near the Mongolian border in China and its implications for continental growth. Acta Petrologica Sinica 22(5):1267–1278 (Chinese with English abstract)

Tong Y, Wang T, Hong DW, Dai YJ, Han BF, Liu XM (2007) Ages and origin of the early Devonian granites from the north part of Chinese Altai Mountains and its tectonic implications. Acta Petrologica Sinica 23(8):1933–1944 (Chinese with English abstract)

Turner SP, Foden JD, Morrison RS (1992) Derivation of some A-type magmas by fractionation of basaltic magma: an example from the Padthaway Ridge, South Australia. Lithos 28(2):151–179. doi:10.1016/0024-4937(92)90029-X

Wang ZG, Zhao ZH (1998) Origin and evolution of the granitoids in Altay. Geological Publishing House, Beijing Geoscience of Xinjiang, vol 1, pp 69–77 (Chinese)

Wang T, Hong DW, Tong Y, Han BF, Shi YR (2005) Zircon SHRIMP U–Pb age and origin of post-orogenic Lamazhou granitic pluton from Chinese Altai Orogen: its implications for vertical continental growth. Acta Petrologica Sinica 21(3):640–650 (Chinese with English abstract)

Wang T, Hong DW, Jahn BM, Tong Y, Wang YB, Han BF, Wang XX (2006) Timing, petrogenesis, and setting of Paleozoic synorogenic intrusions from the Altai Mountains, Northwest China: implications for the tectonic evolution of an accretionary orogen. J Geol 114(6):735–751. doi:10.1086/507617

Wang T, Tong Y, Jahn BM, Zou TR, Wang YB, Hong DW, Han BF (2007) SHRIMP U–Pb zircon geochronology of the Altai no. 3 Pegmatite, NW China, and its implications for the origin and tectonic setting of the pegmatite. Ore Geol Rev 32(1–2):325–336. doi:10.1016/j.oregeorev.2006.10.001

Wang T, Jahn BM, Kovach VP, Tong Y, Hong DW, Han BF (2009) Nd–Sr isotopic mapping of the Chinese Altai and implications for continental growth in the Central Asian Orogenic Belt. Lithos 110(1–4):359–372. doi:10.1016/j.lithos.2009.02.001

Whalen JB, Currie KL, Chappell BW (1987) A-type granites: geochemical characteristics, discrimination and petrogenesis. Contrib Mineral Petrol 95(4):407–419. doi:10.1007/BF00402202

Williams IS (1998) U–Th–Pb geochronology by ion microprobe. In: McKibben MA, Shanks III WC, Ridley WI (eds) Applications of microanalytical techniques to understanding mineralizing processes. Reviews in Economic Geology, vol 7, pp 1–35

Windley BF, Kröner A, Guo JH, Qu GS, Li Y, Zhang C (2002) Neoproterozoic to Palaeozoic geology of the Altai orogen, NW China: new zircon age data and tectonic evolution. J Geol 110:719–737. doi:10.1086/342866

Windley BF, Alexeiev D, Xiao WJ, Kröner A, Badarch G (2007) Tectonic models for accretion of the Central Asian Orogenic Belt. J Geol Soc Lond 164(1):31–47. doi:10.1144/0016-76492006-022

Xiao WJ, Windley BF, Hao J, Zhai MG (2003) Accretion leading to collision and the Permian Solonker suture, Inner Mongolia, China: termination of the central Asian orogenic belt. Tectonics 22(6):1069. doi:10.1029/2002TC001484

Xiao WJ, Windley BF, Badarch G, Sun S, Li J, Qin KZ, Wang ZH (2004) Palaeozoic accretionary and convergent tectonics of the southern Altaids: implications for the lateral growth of Central Asia. J Geol Soc Lond 161(3):339–342. doi:10.1144/0016-764903-165

Xiao WJ, Han CM, Yuan C, Chen HL, Sun M, Lin SF, Li ZL, Mao QG, Zhang JE, Sun S, Li JL (2006) Unique Carboniferous-Permian tectonic-metallogenic framework of Northern Xinjiang (NW China): constraints for the tectonics of the southern Paleoasian Domain. Acta Petrologica Sinica 22(5):1362–1376 (Chinese with English abstract)

Xiao WJ, Pirajno F, Seltmann R (2008a) Geodynamics and metallogeny of the Altaid orogen. J Asian Earth Sci 32(2–4):77–81. doi:10.1016/j.jseaes.2007.10.003

Xiao WJ, Han CM, Yuan C, Sun M, Lin SF, Chen HL, Li ZL, Li JL, Sun S (2008b) Middle Cambrian to Permian subduction-related accretionary orogenesis of Northern Xinjiang, NW China: implications for the tectonic evolution of central Asia. J Asian Earth Sci 32(2–4):102–117. doi:10.1016/j.jseaes.2007.10.008

Xu JF, Chen FR, Yu XY, Niu HC, Zheng ZP (2001) Kuerti ophiolite in Altay area of north Xinjiang: magmatism of an ancient back-arc basin. Acta Petrologica Et Mineralogica 20(3):344–352 (Chinese with English abstract)

Yakubchuk A (2004) Architecture and mineral deposit settings of the Altaid orogenic collage: a revised model. J Asian Earth Sci 23:761–779. doi:10.1016/j.jseaes.2004.01.006

Yang FQ, Mao JW, Yan SH, Liu F, Chai FM, Zhou G, Liu GR, He LX, Gen XX, Dai JZ (2008) Geochronology, geochemistry and geological implications of the Mengku synorogenic plagiogranite pluton in Altay, Xinjiang. Acta Geologica Sinica 82(3):485–499 (Chinese with English abstract)

Yuan C, Sun M, Xiao WJ, Li XH, Lin SF, Xia XP, Long XP, Cai KD (2006) Palaeozoic accretion of Chinese Altai: geochronological constraints from granitoids. Abstract of Western Pacific Geophysics Meeting, CD-ROM, Beijing

Yuan C, Sun M, Xiao WJ, Li XH, Chen HL, Lin SF, Xia XP, Long XP (2007) Accretionary orogenesis of the Chinese Altai: insights from Palaeozoic granitoids. Chem Geol 242(1–2):22–39. doi: 10.1016/j.chemgeo.2007.02.013

Zhang JH, Wang JB, Ding RF (2000) Characteristics and U-Pb ages of zircon in metavolcanics from the Kangbutiebao Formation in the Altay orogen, Xinjiang. Regional Geology of China 19(3):281–287 (Chinese with English abstract)

Zhang HY, Niu HC, Terada K, Yu XY, Sato H, Ito J (2003) Zircon SHRIMP U–Pb dating on plagiogranite from Kuerti ophiolite in Altay, North Xinjiang. Chin Sci Bull 48(20):2231–2235

Zhang ZC, Yan SH, Chen BL, Zhou G, He YK, Chai FM, He LX, Wan YS (2006) SHRIMP zircon U–Pb dating for subduction-related granitic rocks in the northern part of east Junggar, Xinjiang. Chin Sci Bull 51(8):1565–1574

Zhang ZC, Zhou G, Yan SH, Chen BL, He YK, Chai FM, He LX (2007) Geology and geochemistry of the late Paleozoic volcanic rocks of the south margin of the Altai Mountains and implications for tectonic evolution. Acta Geologica Sinica 81(3):344–358 (Chinese with English abstract)

Zhao ZH, Wang ZG, Zou TR, Masuda A (1993) The REE, isotopic composition of O, Pb, Sr and Nd and petrogenesis of granitoids in the Altai region. In: Tu Guangzhi (ed) Progress of solid-earth sciences in northern Xinjiang, China Science Press, Beijing 239–266 (Chinese with English abstract)

Zhao XF, Zhou MF, Li JW, Wu FY (2008) Association of Neoproterozoic A- and I-type granites in South China: implications for generation of A-type granites in a subduction-related environment. Chem Geol 257:1–15. doi:10.1016/j.chemgeo.2008.07.018

Zhou G, Zhang ZC, Luo SB, He B, Wang X, Yin LJ, Zhao H, Li AH, He YK (2007a) Confirmation of high temperature strongly peraluminous Mayin'ebo granites in the south margin of Altay, Xinjiang: age, geochemistry and tectonic implications. Acta Petrologica Sinica 23(8):9–20 (Chinese with English abstract)

Zhou G, Zhang ZC, Wang X, Luo SB, He B, Zhang XL (2007b) Zircon U–Pb SHRIMP and ^{40}Ar-^{39}Ar dating of the granitic mylonite in the Mayinebo fault belt of north Xinjiang and its geological significance. Acta Geologica Sinica 81(3):359–369 (Chinese with English abstract)

Zou TR, Cao HZ, Wu BQ (1989) Orogenic and anorogenic granitoids of Altay Mountains of Xinjiang and their discrimination criteria. Acta Geol Sinica 2(1):45–64